Journal of Magnetic Resonance 204 (2010) 21–25

Contents lists available at ScienceDirect

Journal of Magnetic Resonance

journal homepage: www.elsevier.com/locate/jmr

Measurement of vorticity diffusion by NMR microscopy

Jennifer R. Brown *, Paul T. Callaghan

Victoria University of Wellington, School of Chemical and Physical Sciences, The MacDiarmid Institute of Advanced Materials and Nanotechnology, PO Box 600, Wellington 6012, New Zealand

ARTICLE INFO

Article history:
Received 23 November 2009
Revised 20 January 2010
Available online 1 February 2010

Keywords:
NMR
Vorticity diffusion
Velocimetry
RARE

ABSTRACT

In a Newtonian fluid, vorticity diffuses at a rate determined by the kinematic viscosity. Here we use rapid NMR velocimetry, based on a RARE sequence, to image the time-dependent velocity field on startup of a fluid-filled cylinder and therefore measure the diffusion of vorticity. The results are consistent with the solution to the vorticity diffusion equation where the angular velocity on the outside surface of the fluid, at the cylinder's rotating wall, is fixed. This method is a means of measuring kinematic viscosity for low viscosity fluids without the need to measure stress.

1. Introduction

A fluid is a material that deforms continuously when subjected to a shearing stress. In contrast with solids, where deformation determines stress, it is the rate of deformation that counts in fluids. The measure of deformation is known as strain. In fluid mechanics, even the simplest of flows often combine both strain and rotation, the measure of rotational motion in a fluid being the vorticity $w = \nabla \times v$. However, while deformation of a fluid implies the presence of a velocity gradient, since a point in the material is moving relative to another point, a velocity gradient is not always indicative of a deformation. For example, purely rotational motion, such as that in a rigid solid, demonstrates a velocity gradient in the absence of deformation. Flows where the vorticity is everywhere zero (irrotational or potential flows) represent another special case where deformation is possible in the absence of rotation. In this paper, we shall be concerned with the migration of vorticity across a fluid, a process that is governed by diffusion, and we show that NMR provides a means of measuring this diffusion phenomenon. In demonstrating this process we shall follow the evolution of the flow field from an initial condition, where the vorticity is limited to the boundary of a stationary fluid, to a final state where the vorticity has equilibrated across the fluid, resulting in a purely rotational flow in which the vorticity is everywhere constant. The chosen geometry is that of a fluid-filled cylinder, initially at rest, but with a step change in angular velocity of the cylinder wall imposed at startup.

According to Kelvin's circulation theorem [1], the basis of potential flow theory, an incompressible fluid vorticity free at an instant in time should remain so at any time. However, motion at a boundary can act as a source of external vorticity. A stationary fluid, initially vorticity free, when exposed to shearing forces will become contaminated with vorticity at the fluid boundaries and a velocity field develops. In the case considered here, fluid is contained within a cylinder initially at rest. Upon sudden rotation of the cylinder, frictional shear stresses occur at the solid–fluid interface and exert a torque upon the adjacent fluid layer, causing it to accelerate. This torque effectively "diffuses" along the radial dimension until the fluid velocity reaches the familiar steady state rigid body rotation linear velocity field. The appropriate dynamical description is that of vorticity diffusion [1], as governed by a standard diffusion equation

$$\frac{\partial w}{\partial t} = \frac{\eta}{\rho}\nabla^2 w \tag{1}$$

where the kinematic viscosity η/ρ is effectively a diffusion coefficient. In our experiment, MRI measurements of the velocity field provide a window on the diffusion process. In order to have the necessary time resolution, pulsed gradient spin–echo (PGSE) encoded RARE imaging has been used to acquire spatially resolved measurements of the fluid velocity field within 2 s. Due to the enhanced temporal resolution of the velocity images, it is possible to directly monitor the development of the velocity gradient to a steady state, and thereby the diffusion of vorticity. We directly compare our velocimetry results with the predictions of the vorticity diffusion equation. A simple Newtonian fluid with low kinematic viscosity, acetone, is compared with water and low molecular weight polydimethylsiloxane, a shear thinning fluid that is Newtonian under

* Corresponding author. Fax: +64 04 463 5237.
E-mail addresses: jbrown@coe.montana.edu (J.R. Brown), paul.callaghan@vuw.ac.nz (P.T. Callaghan).

1090-7807/$ - see front matter © 2010 Elsevier Inc. All rights reserved.
doi:10.1016/j.jmr.2010.01.011

the conditions in this study. These results provide a nice demonstration of fundamental fluid mechanics. They also suggest a means of measuring fluid viscosity via NMR velocimetry without the need to measure the fluid stress, although this is by way of a curiosity and not suggested as a practical and economical alternative to simpler benchtop methods.

2. Vorticity diffusion in a cylinder

For a fluid contained in a cylinder at startup rotation, the relevant vorticity diffusion equation uses cylindrical polar coordinates (r, θ, z). For an infinite cylinder of radius a, there is no z or θ dependence of the velocity and so the diffusion equation becomes

$$\frac{\partial w}{\partial t} = \frac{\eta}{\rho}\left[\frac{\partial^2 w}{\partial r^2} + \frac{1}{r}\frac{\partial w}{\partial r}\right] \tag{2}$$

The vorticity, dependent upon both radial position and time, can be separated into two functions which depend only upon one variable each, $w(r,t) = u(r)T(t)$, reducing the partial differential equation to two ordinary differential equations. These equations may be set equal to the same constant, chosen for convenience as $-\alpha^2 D$, where the "diffusion coefficient" $D = \eta/\rho$, is the kinematic viscosity [2].

$$\frac{1}{T(t)}\frac{dT(t)}{dt} = -\alpha^2 D; \quad \frac{D}{u(r)}\left[\frac{d^2u(r)}{dr^2} + \frac{1}{r}\frac{du(r)}{dr}\right] = -\alpha^2 D \tag{3}$$

The general solution is then

$$w(r,t) = u(r)\exp(-\alpha^2 Dt) \tag{4}$$

where $\frac{d^2u(r)}{dr^2} + \frac{1}{r}\frac{du(r)}{dr} + \alpha^2 u(r) = 0$ is a Bessel's equation of zeroth order. After non-dimensionalization of the eigenvalues α by the cylinder radius a, the solution of this equation requires a Bessel function of the first kind, the solution of the second kind being infinite at $r = 0$ with the $\beta = a\alpha$ eigenvalues consistent with the boundary conditions [3]. Therefore,

$$w(r,t) = \sum_{n=1}^{\infty} A_n J_0(\beta_n r/a)\exp\left(-\frac{\beta_n^2 Dt}{a^2}\right) \tag{5}$$

In order to use the vorticity diffusion process to monitor the behavior of the fluid, we need to know the boundary condition. At the fluid wall, the boundary condition is more easily described from the standpoint of the constant fluid velocity at the cylinder surface under the non-slip condition. At $r = a$, the fluid assumes the maximum velocity of the rotating cylinder $v_{\max} = a\Omega$ where Ω is the applied fixed angular velocity. For this reason, and because the velocity field may be directly measured by NMR, we integrate the vorticity to yield the spatio-temporal velocity dependence. The initial and final states of the fluid velocity are known and provide a means of getting the exact solution.

Since the relationship between vorticity and velocity is $w = \nabla \times v$,

$$w = \frac{1}{r}\frac{\partial(rv)}{\partial r} \tag{6}$$

where the direction of the vorticity vector is along the axis of the cylinder. The conversion from $w(r,t)$ to $v(r,t)$ is based on integration using Eq. (6).

Imposing the condition that $v(r) = \frac{v_{\max} r}{a}$ as $t \to \infty$ results in a general solution

$$v(r,t) = \frac{v_{\max}}{a}r - a\sum_{n=1}^{\infty}\frac{A_n}{\beta_n}J_1(\beta_n r/a)\exp\left(-\frac{\beta_n^2 Dt}{a^2}\right) \tag{7}$$

At $r = a$, the velocity $v(r)$ must go to the maximum velocity at the rotating wall of the cylinder, $v(a) = v_{\max}$. To satisfy these conditions, the β_n must be roots of $J_1(\beta_n) = 0$ [4]. Now to solve for the Bessel coefficients A_n, the condition that at $t = 0$, $v(r) = 0$ for all $0 < r < a$ results in the velocity equation

$$\frac{v_{\max}}{a}r = a\sum_{n=1}^{\infty}\frac{A_n}{\beta_n}J_1(\beta_n r/a) \tag{8}$$

Eq. (8) leads to the Bessel coefficient (see Appendix)

$$A_n = -\frac{2v_{\max}}{a}\frac{J_0(\beta_n)}{J_2^2(\beta_n)} \tag{9}$$

and the velocity equation is

$$v(r,t) = \frac{v_{\max}}{a}r - 2v_{\max}\sum_{n=1}^{\infty}\exp\left(-\frac{\beta_n^2 Dt}{a^2}\right)\frac{J_0(\beta_n)J_1(\beta_n r/a)}{\beta_n J_2^2(\beta_n)} \tag{10}$$

The vorticity obtained by derivation then is

$$w(r,t) = \frac{2v_{\max}}{a} - \frac{2v_{\max}}{a}\sum_{n=1}^{\infty}\exp\left(-\frac{\beta_n^2 Dt}{a^2}\right)\frac{J_0(\beta_n)J_0(\beta_n r/a)}{J_2^2(\beta_n)} \tag{11}$$

3. Experimental methods and materials

To monitor the transient vorticity diffusion, a rapid NMR velocimetry technique was necessary. The velocity measurements were made using an adaptation of a RARE rapid imaging sequence [5]. A PGSE gradient pair encoding for displacement is applied first, then followed by a RARE CPMG train of slice-selective 180° radio frequency pulses wherein frequency and phase encoding is used to encode spatially in two dimensions. The entire k-space raster is therefore collected within one excitation and in minimal time and the Fourier transform is a 2D image over a slice. The pulsed gradient pair of amplitude g and duration δ separated by an observation time Δ [6–8] impart a phase to the NMR signal $\phi = \exp(-i2\pi qz)$, where $q = \frac{1}{2\pi}\gamma\delta g_z$, that relates to the displacement z in the applied gradient direction. The Fourier transform of the signal with respect to q yields the propagator, or average probability distribution of spin displacement $\overline{P}(z,\Delta)$, in each pixel of the 2D image. While 24 echoes were collected, only the even echoes of the echo train were retained in order to eliminate ghosting artifacts in the image related to flow. The pulse sequence is shown in Fig. 1. A slice of 4 mm thickness is selected along the vorticity axis of the cylinder. Frequency encoding as applied in the radial direction, resulting in a spatial resolution of 59 μm in the region of interest across the cylinder, while phase encoding was along the vorticity axis for a coarse spatial resolution of 7.5 mm where the velocity did not change. Two velocity encoding gradient steps ($q = 0$ and $q \neq 0$) were used, to keep the image acquisition time short. The displacement-induced phase shift between the pixels of the $q = 0$ and $q \neq 0$ images is a measure of the average velocity over the time Δ, which was 10 ms in our experiment. Velocity values are obtained by zero filling images for remaining q values and

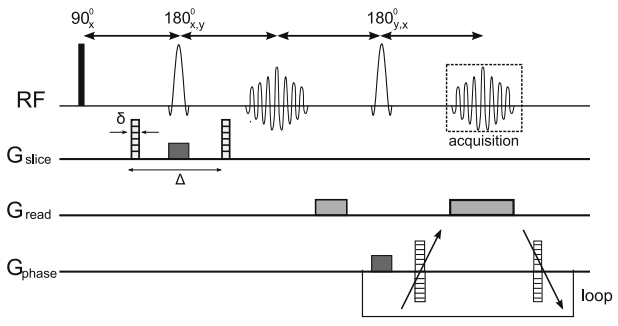

Fig. 1. RARE velocity imaging pulse sequence.

then Fourier transforming with respect to q. Thus, one obtains a displacement distribution convolved with the spectrum of a hat function. The maximum of this function corresponds to the displacement of spins over the encoding period Δ and so the velocity may be determined. The primary factor limiting the temporal resolution is the repetition time. The repetition time was 750 ms, chosen as the shortest possible before image quality was adversely effected by signal losses due to incomplete longitudinal (T_1) relaxation.

The NMR measurements were conducted on a Bruker AVANCE400 spectrometer with a 9.4 T superconducting 89 mm vertical bore magnet, Micro 2.5 imaging probe capable of producing maximum gradients of 15 G/mm with a Bruker GREAT-60 power supply and 25 mm diameter rf coil. Data were acquired using the Bruker software package Topspin and analyzed with Prospa (Magritek, Wellington, New Zealand) and Matlab® software. The cylinder was a standard glass NMR tube of 18 mm inner diameter. The cylinder rested inside a larger diameter NMR tube, with Teflon spacers in the gap between cylinders in order to ensure smooth rotation of the inner cylinder. A drive shaft assembly connects the inner glass cylinder with a stepper motor drive system that sits on top of the magnet and rotates the tube at a fixed frequency. The time to reach the preset rotation speed on startup was approximately 0.5 s. The fluids used were acetone with a kinematic viscosity at 20 °C of 0.41 cSt, water at 1 cSt, and polydimethylsiloxane (MW = 5200) which has a high kinematic viscosity of approximately 95 cSt.

4. Results and discussion

The analytical solution at several points in time of the vorticity in a cylinder abruptly rotated is shown in Fig. 2, where acetone is the fluid in the cylinder. As the cylinder begins to rotate, the fluid at the solid–liquid boundary of the cylinder glass wall adheres to the surface, which then drags the fluid along as it rotates. The fluid boundary layer exerts a stress on the next fluid layer, thereby contaminating the fluid near the wall with vorticity. For the rotating cylinder geometry considered here, vorticity at the wall boundary is positive and negative in the center. With increasing time, vorticity diffuses throughout the tube becoming constant, the viscosity of the solution begins to dominate rather than inertia and the velocity profile reaches the familiar linear steady state solid body rotation. In contrast, for the case of laminar fluid flow through a cylinder, classic Poiseuille flow, vorticity would be positive at one wall and negative on the other, annihilating at the center.

Fig. 3 shows the full solution $w(r,t)$ across the cylinder radius from $t = 0$ to 128 s. The colorscale is related to the vorticity magnitude. Fig. 3a shows a side view, where the vorticity across the cylinder diameter as shown in Fig. 2 is visible. In Fig. 3b, the dataset is rotated to highlight the timescale of the vorticity diffusion.

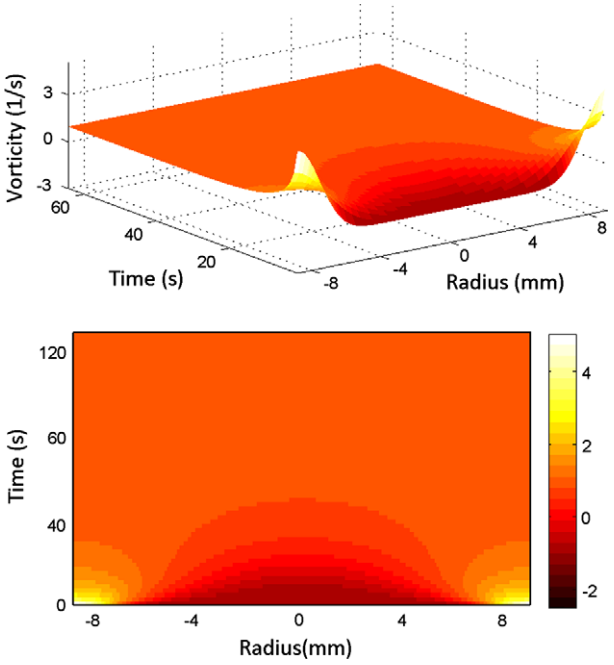

Fig. 3. Solution for the vorticity across the diameter of an abruptly rotated cylinder with increasing time, demonstrating the diffusion of vorticity.

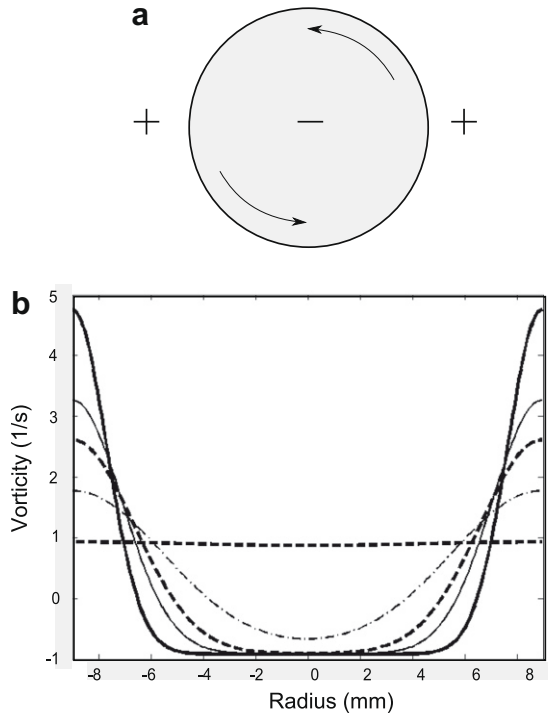

Fig. 2. (a) A cylinder abruptly rotated has positive vorticity at the solid–fluid boundary of the cylinder wall and negative vorticity in the cylinder center. (b) The analytical solution for the vorticity across the cylinder diameter evolves with increasing time as the vorticity diffuses throughout the cylinder, until it reaches a constant steady state value. $t = 2$ s (thick line), 4 s (thin line), 6 s (thick dashed line), 12 s (thin dash-dot line) and 32 s (dotted line).

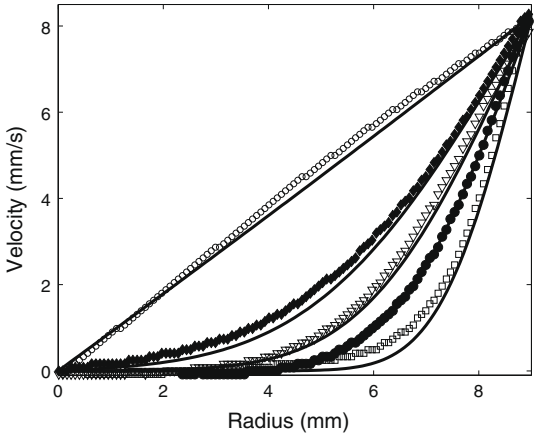

Fig. 4. Velocity $v(r,t)$ from the center of the cylinder to the outer rotating wall with increasing time. The solution (lines) matches the data (symbols) well. $t = 2$ s (open squares), 4 s (closed circles), 6 s (open triangles), 10 s (closed diamonds) and 64 s (open circles).

Since the solution is exact, there are no unknown parameters. The data and the solution should match exactly, with a coefficient equal to kinematic viscosity of the selected fluid. The rate of diffusion depends only upon the kinematic viscosity of the fluid, while the cylinder rotation rate affects only the boundary condition. Even then it only determines the value of the maximum velocity at the wall, which does not impact the time evolution of the vorticity. Fig. 4 shows a comparison of the velocity field solution for acetone compared to the RARE velocity imaging data with increasing time as the cylinder starts rotation.

The lines are not in exact agreement, likely due to the ~0.5 s time to startup and the 750 ms time averaging inherent to the RARE data, resulting in a consequent delay between velocity and position encoding. Despite this temporal blurring and small distortion of the effective experimental timescale, the fluid behavior is accurately captured. When the kinematic viscosity in the solution was varied to get the best fit of the data in Fig. 4, the variation from literature values for acetone was found to be ~10%. The RARE velocity images also have some noise variations, but the agreement between the analytical solution and the velocity imaging data is still remarkably good, as demonstrated again in Fig. 5. The three-dimensional dataset is represented with a color scale this time related to velocity. Fig. 5a shows the side view of the velocity gradient across the cylinder diameter as shown in Fig. 4, and in Fig. 5b the dataset is rotated to highlight the timescale of the vorticity diffusion as the velocity profile changes shape until reaching the steady state form.

Fig. 6 clearly shows the difference in the vorticity diffusion timescale depending upon kinematic viscosity. From left to right, acetone has the lowest kinematic viscosity of 0.41 cSt followed by water at 1 cSt and finally a low molecular weight polydimethylsiloxane (PDMS) at 95 cSt. For PDMS, the diffusion of vorticity is so fast that the velocity field reaches a steady state within the two seconds of the first RARE image.

5. Conclusion

NMR RARE rapid velocimetry has provided the means to measure vorticity diffusion via the spatio-temporal evolution of the velocity profile. Vorticity diffusion is a fundamental fluid mechanical concept difficult to measure by experiment, but through the enhanced temporal resolution achieved from the combination of PGSE and RARE imaging, good agreement was found between data and the solution to the vorticity diffusion equation. These results

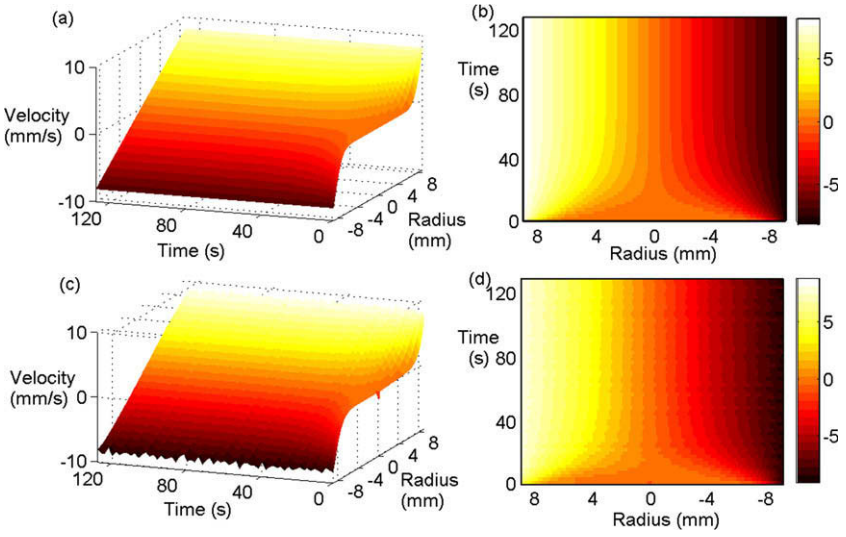

Fig. 5. (a and b) Analytical solution for the velocity $v(r,t)$, where acetone is the fluid in the rotating cylinder. (c and d) RARE velocity imaging data for $v(r,t)$ of acetone. The maximum velocity at the rotating glass wall is 8.24 mms^{-1}.

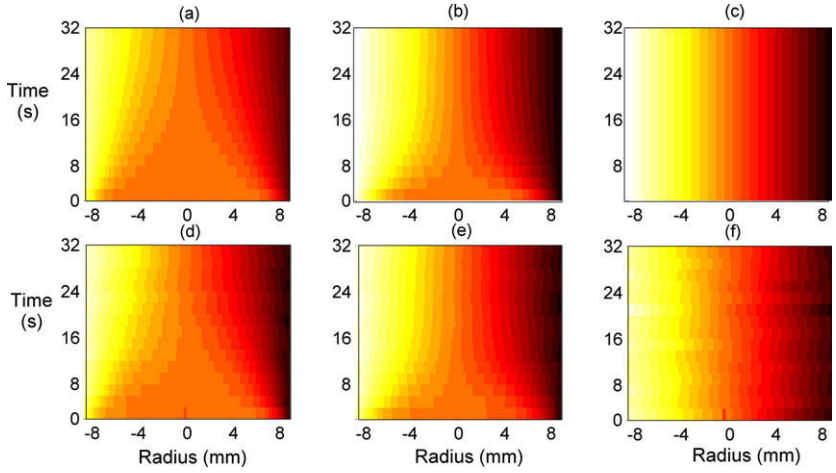

Fig. 6. The analytical velocity field solution for (a) acetone, (b) water and (c) PDMS (MW ~ 5200). The RARE velocity imaging data are (d), (e) and (f) for acetone, water and PDMS respectively. In all fluids, the velocity field reaches a nearly steady state within the first 32 s after beginning rotation of the cylinder.

also demonstrate how RARE velocimetry could be used to measure fluid viscosity of low viscosity fluids by the time-dependent velocity alone, without the need for stress measurement.

Appendix A

To solve for the Bessel coefficients A_n the condition that at $t = 0$, $v(r) = 0$ for all $0 < r < a$ results in the velocity equation

$$\frac{v_{\max}}{a} r = a \sum_{n=1}^{\infty} \frac{A_n}{\beta_n} J_1(\beta_n r/a) \tag{A.1}$$

Multiplying both sides of the equation by $rJ_1(\beta_m r/a)$ and integrating from 0 to a,

$$\frac{v_{\max}}{a} \int_0^a r^2 J_1(\beta_m r/a) dr = a \int_0^a r \frac{A_n}{\beta_n} J_1(\beta_m r/a) J_1(\beta_n r/a) dr \tag{A.2}$$

From the orthogonality relation for Bessel functions [3], the right hand side of Eq. (A.2) is

$$a \int_0^a r \frac{A_n}{\beta_n} \left[J_1^2 \left(\frac{\beta_n r}{a} \right) \right] dr = \frac{A_n}{\beta_n} \left[\frac{a^3}{2} J_2^2(\beta_n) \right] \tag{A.3}$$

Using the identity $J_1(\beta) = -J_0'(\beta)$ the left hand side of the Eq. (A.2) is solved through integration by parts,

$$\frac{v_{\max}}{a} \int_0^a r^2 J_1(\beta_m r/a) dr = -\frac{v_{\max} a^2}{\beta_n} J_0(\beta_n) \tag{A.4}$$

The Bessel coefficient is then

$$A_n = -\frac{2 v_{\max}}{a} \frac{J_0(\beta_n)}{J_2^2(\beta_n)} \tag{A.5}$$

References

[1] T.E. Faber, Fluid Dynamics for Physicists, Cambridge University Press, Cambridge, 1995.
[2] J. Crank, The Mathematics of Diffusion, Clarendon Press, Oxford, 1975.
[3] H.S. Carslaw, J.C. Jaeger, Conduction of Heat in Solids, Oxford University Press, London, 1959.
[4] A. Gray, G.B. Mathews, A Treatise on Bessel Functions and their Applications to Physics, Macmillan, London, 1922.
[5] P. Galvosas, P.T. Callaghan, Fast magnetic resonance imaging and velocimetry for liquids under high flow rates, Journal of Magnetic Resonance 181 (2006) 119–125.
[6] P.T. Callaghan, Principles of Nuclear Magnetic Resonance Microscopy, Oxford University Press, New York, 1991.
[7] J.D. Seymour, P.T. Callaghan, Generalized approach to NMR analysis of flow and dispersion in porous medium, AIChE Journal 43 (1997) 2096–2111.
[8] J. Stepisnik, Measuring and imaging of flow by NMR, Progress in NMR Spectroscopy 17 (1985) 187–209.